STATISTICAL MODELLING AND ANOVA ANALYSIS OF THERMAL CONTACT RESISTANCE IN SOLID-SOLID INTERFACES

Rachid CHADOULI[1], Smain BENYAMINA[2], Salem MERABTI[3], Abdellah BOUDINA[4]*

[1]*Laboratory of Fluid Industrials, Measures & Application (FIMA), M*echanical Engineering Department, Faculty of Science and Technology, University of Khemis-Miliana, Algeria

[2,3]Laboratory of Acoustics and Civil Engineering, Faculty of Science and Technology, University Djilali Bounaama of Khemis-Miliana, Algeria

[4] *Laboratory of Fluid Industrials, Measures & Application (FIMA), Faculty of Science and Technology, University Djilali Bounaama of Khemis-Miliana, 44225, Algeria*

[*] Corresponding author; E-mail: s.merabti@univ-dbkm.dz

Thermal contact resistance (TCR) limits interfacial heat transfer in solid–solid junctions and depends on several parameters, including surface condition and the thermophysical properties of the contacting materials. This study quantitatively evaluates the influence of material pairing (steel/steel, steel/copper, steel/nickel) and contact surface area (five levels: 0.05–0.8 mm²) on TCR and heat flux using a two-way analysis of variance (ANOVA) with interaction (n = 45). The results indicate that the contact surface area is the dominant factor affecting TCR ($p < 0.001$*; 89.2% of the total variance), whereas the material type constitutes the primary factor governing heat flux (*$p < 0.001$*). A robust linear regression model (*$R^2 = 0.96$*) further confirms these trends. These findings provide a statistically sound framework for the optimization of thermal interfaces in power electronics applications, highlighting the superior performance of the steel/copper material pair.*

Keywords*: Thermal contact resistance (TCR), Contact surface area, Two-way ANOVA, Heat flux and Statistical modeling.*

1. Introduction

In many modern industrial and technological systems, the efficiency of heat transfer is a critical concern, particularly in high-power electronic devices, heat exchangers, mechanical joints, and structures subjected to significant thermal gradients [1]. When two solids are brought into contact, heat transfer across their interface is inherently imperfect due to the presence of microscopic surface irregularities and, in some cases, intermediate layers [2, 3]. This thermal discontinuity is characterized by a key physical parameter known as thermal contact resistance (TCR) [4].

TCR represents the limitation of heat flux at the interface between two contacting solids, even when the individual materials exhibit high thermal conductivity. This phenomenon is especially pronounced under unsteady conditions involving vibration, where thermal fluctuations depend on surface topography and mechanical deformation, as recently modeled by Zhao et al. [5] using a

multiphysics approach. Consequently, TCR is a decisive parameter in the analysis, modeling, and optimization of thermal interface performance [6, 7].

Controlling thermal contact resistance has become increasingly important in the current context of system miniaturization, higher operating speeds, and increased power density. Thermal interface materials (TIMs), such as polymer composites filled with graphene or boron nitride, are widely employed to reduce contact resistance by enhancing thermal conductivity (>10 W/m·K), minimizing bond-line thickness (<10 µm), and improving interfacial wetting through chemical or nanostructured surface treatments. Emerging self-healing and phase-change TIMs offer promising solutions for high-power electronics and advanced thermal management applications [8]. In electronic devices, for instance, the continuous increase in power density necessitates rigorous thermal control to prevent degradation, efficiency loss, or component failure [9]. Similarly, in mechanical applications such as fastening systems, brakes, bolted joints, or structural interfaces, inadequate heat dissipation may lead to differential thermal expansion, additional stresses, or even premature material failure [10]. Therefore, the ability to accurately quantify and predict thermal contact resistance is essential to ensure the reliability, durability, and energy optimization of thermomechanical systems [11].

Thermal contact resistance strongly depends on a range of intrinsic and extrinsic factors. At the microscopic scale, surface roughness, flatness, and microgeometry govern the real area of contact, which is significantly smaller than the apparent contact area [12]. From a material perspective, thermal conductivity, hardness, mechanical properties, and coefficients of thermal expansion influence the interface's capacity to transmit heat [13, 14]. Moreover, parameters such as contact pressure, the presence of interfacial films (e.g., oxides, lubricants, or contaminants), local temperature, and surface treatment conditions can substantially alter the thermal behavior of the interface [15]. This multiplicity of influencing factors explains why the evaluation of TCR remains a complex issue, requiring reliable experimental methods as well as analytical or statistical approaches capable of systematically modeling its evolution [16].

Over the past decades, several theoretical models have been proposed to explain the mechanisms governing thermal contact resistance [17], notably the models developed by Cooper et al. [13], which are based on heat conduction through micro-contacts. Although these models have provided valuable analytical relationships, their application often relies on simplifying assumptions regarding asperity geometry, pressure distribution, or material properties [18]. More recently, advanced numerical approaches have been developed to model thermal contact resistance at the interface between dissimilar materials [19, 20], explicitly accounting for surface irregularities and thermal discontinuities. For example, an efficient numerical model based on diffuse interface and immersed boundary methods has been proposed to incorporate contact resistance into multimaterial simulations. This model considers both steady-state and transient conduction regimes, thereby improving the accuracy of temperature jump predictions at the interface and enhancing the multiphysics representation of heat transfer across complex interfaces [21, 22]. In practice, however, industrial interfaces are rarely ideal [23, 24], and the discrepancy between theoretical models and real behavior justifies the growing interest in statistically driven approaches based on experimental data analysis [25].

Advanced statistical tools, such as two-way ANOVA and multiple linear regression, provide a powerful alternative to purely theoretical models by accurately quantifying the effects of contact surface area and material pairing (steel/steel, steel/copper, steel/nickel) on thermal contact resistance,

while explicitly accounting for their interactions. The present study addresses this gap in the literature by developing a robust predictive model ($R^2 \approx 0.96$) derived from statistical analysis, enabling the establishment of a precise predictive equation for TCR and supporting the optimization of thermal interfaces to minimize contact resistance.

2. Materials and Methods

2.1. Finite element modeling of TCR

The numerical simulations presented in this work are based on a two-dimensional steady-state heat transfer model formulated using the Finite Element Method and executed with ABAQUS software (version 6.14). Before the main calculations, a mesh convergence study was performed in order to achieve an appropriate compromise between solution accuracy and computational cost. The selected mesh employs conventional linear quadrilateral heat transfer elements (DC2D4).

A structured meshing approach was adopted, along with a mesh transition control technique to limit element distortion. According to this discretization, the computational domain is composed of 27,375 finite elements.

The model considers two solid bodies in thermal contact, both having identical geometrical dimensions, with a height of 8 cm and a width of 2 cm. The contacting interfaces are assumed to be rough and are idealized by uniformly distributed square asperities, characterized by an average surface roughness of Ra = 20 μm and a constant asperity spacing. The effective contact area is taken as 10% of the apparent contact area. The thermal conductivity of the solid materials ranges from 20 to 390 $W \cdot m^{-1} \cdot K^{-1}$, while the interfacial gap is represented by an equivalent medium with thermal conductivity values varying between 0.16 and 5 $W \cdot m^{-1} \cdot K^{-1}$.

To compute the interface temperatures (T_{ch} and T_f, shown in Fig. 1), determine the heat flux q, and evaluate the thermal contact resistance, fixed temperature boundary conditions are applied. The top surface of the upper solid is maintained at 538 K, whereas the bottom surface of the lower solid is set at 338 K. All remaining lateral boundaries are considered thermally insulated.

The thermal contact resistance is defined as:

$$TCR = \frac{T_{ch} - T_f}{q} \tag{1}$$

q: the average heat flow between the two materials in contact:

$$q = \frac{T_{ch} + T_f}{2} \tag{2}$$

$$q = \frac{1}{2}\left[-k_1 S \left(\frac{dT}{dZ}\right)_{ch} - k_1 S \left(\frac{dT}{dZ}\right)_f\right] \tag{3}$$

$$q_{ch} = \frac{k_1 S}{z_{ch}}(T_a - T_{ch}) \tag{4}$$

$$q_f = \frac{k_1 S}{z_b - z_f}\left(T_f - T_b\right) \tag{5}$$

S: is taken to denote the surface which emits the heat flow q

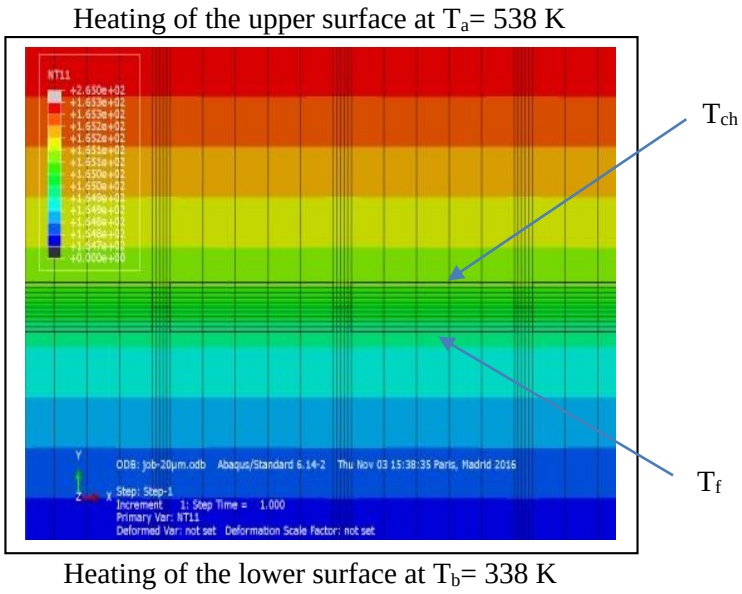

Figure 1. Geometrical model of refined mesh around the contact interface.

Tab. 1 presents the factorial design adopted to investigate thermal contact resistance (TCR) as a function of material pairings and contact surface areas, following the methodology of Chadouli et al. [2]. The design includes three material levels, five surface area levels, and three replicates per combination, resulting in a total of 45 observations (3 × 5 × 3 = 45).

Table 1. Factorial design of the study

Factors	levels	Description
Materials	3	Steel/Steel, Steel/Copper, Steel/Nickel
Surface (mm^2)	5	0.05, 0.2, 0.4, 0.6, 0.8
Replicates	3	Measures repeated for each condition

This study is based on a combined numerical and statistical approach aimed at evaluating the influence of interface parameters on thermal contact resistance (TCR). Three material pairings commonly used in industrial thermal systems were selected: Steel/Steel, Steel/Copper, and Steel/Nickel. For each pairing, multiple configurations were implemented by varying the actual contact surface area, considered a key parameter in interfacial heat transfer. TCR values were determined under controlled conditions to ensure the reliability and consistency of the analysis.

2.2. Statistical model

Analysis of variance (ANOVA) is a statistical method that decomposes the total variability of the data into components attributable to different sources of variation, thereby enabling the assessment of the presence of statistically significant effects.

The two-factor ANOVA model with interaction, suitable for this balanced full factorial design, is expressed as:

$$Y_{ijk} = \mu + \alpha_i + \beta_j + (\alpha\beta)_{ij} + \varepsilon_{ijk}. \qquad (6)$$

Where :

- Y_{ijk}: TCR or heat flux;
- μ: overall average ;
- α_i: material effect i ;
- β_j: surface effect j ;
- $(\alpha\beta)_{ij}$: material/surface interaction;
- ε_{ijk}: error term.

This generalized linear model allows the total variance to be partitioned into additive components (main effects) and multiplicative components (interaction effects), under the classical ANOVA assumptions of normality, homoscedasticity, and independence.

The associated F-tests assess the adequacy of the null hypothesis (H_0: no effect) against the alternative hypothesis (H_1: at least one non-zero effect), with statistical power strengthened by three replicates for each factor-level combination.

With :

- SST: Total sum of squares;

$$SST = \sum_{i=1}^{a}\sum_{j=1}^{b}\sum_{k=1}^{n}(Y_{ijk} - \bar{Y}_{...})^2 \qquad (7)$$

- SS_A: Sum of squares of factor A (Material);

$$SS_A = bn\sum_{i=1}^{a}(\bar{Y}_{i..} - \bar{Y}_{...})^2 \qquad (8)$$

- SS_B: Sum of squares of factor B (Area);

$$SS_B = an\sum_{j=1}^{b}\left(\bar{Y}_{.j.} - \bar{Y}_{...}\right)^2 \qquad (9)$$

- SS_{AB}: Sum of squares of interaction;

$$SS_{AB} = n\sum_{i=1}^{a}\sum_{j=1}^{b}(\bar{Y}_{ij.} - \bar{Y}_{i..} - \bar{Y}_{.j.} + \bar{Y}_{i...})^2 \qquad (10)$$

- SS_{Res}: Residual sum of squares ;

$$SS_{Res} = \sum_{i=1}^{a}\sum_{j=1}^{b}\sum_{k=1}^{n}(Y_{ijk} - \bar{Y}_{ij})^2 \qquad (11)$$

- MS: Medium squares ;

$$MS = \frac{SS}{ddl} \quad (12)$$

- ddl: degrees of freedom ;

ddl = N-1 ; With N = a*b*c = Total number of observations.

- F: Statistical factor ;

$$F = \frac{MS}{MSR_{es}} \quad (13)$$

- p-value: is calculated using Fisher-Snedecor's F distribution.

The null hypotheses tested using the F-statistic of two-factor ANOVA are formulated as follows:

- H_{01}: No effect of material type on TCR;
- H_{02}: No effect of contact surface on TCR;
- H_{03}: No material/surface interaction.

The corresponding alternative hypotheses postulate the existence of at least one non-zero effect within each variance component. The significance level is set to $\alpha = 0.05$, in accordance with standard conventions in materials engineering, ensuring control of the Type I error risk at 5%.

These one-sided tests, based on the F distribution under the classical ANOVA assumptions (normality, homoscedasticity, and independence of errors), allow rejection of H_0 when the associated p-value is less than α. The factorial design ensures adequate statistical power to detect moderate effect sizes (Cohen's $f \approx 0.25$), supported by the use of three replicates per factor combination.

3. Results

The results of the thermal contact resistance (TCR) as a function of contact surface area are presented in Fig. 2. A general decrease in TCR is observed with increasing contact area, regardless of the material combination considered. This trend can be attributed to the enhanced real contact area at the interface, which reduces microscopic gaps and voids that impede heat flow. As the contact area increases, more heat-conducting pathways are established, leading to a lower interfacial thermal resistance, consistent with classical models of thermal contact conduction.

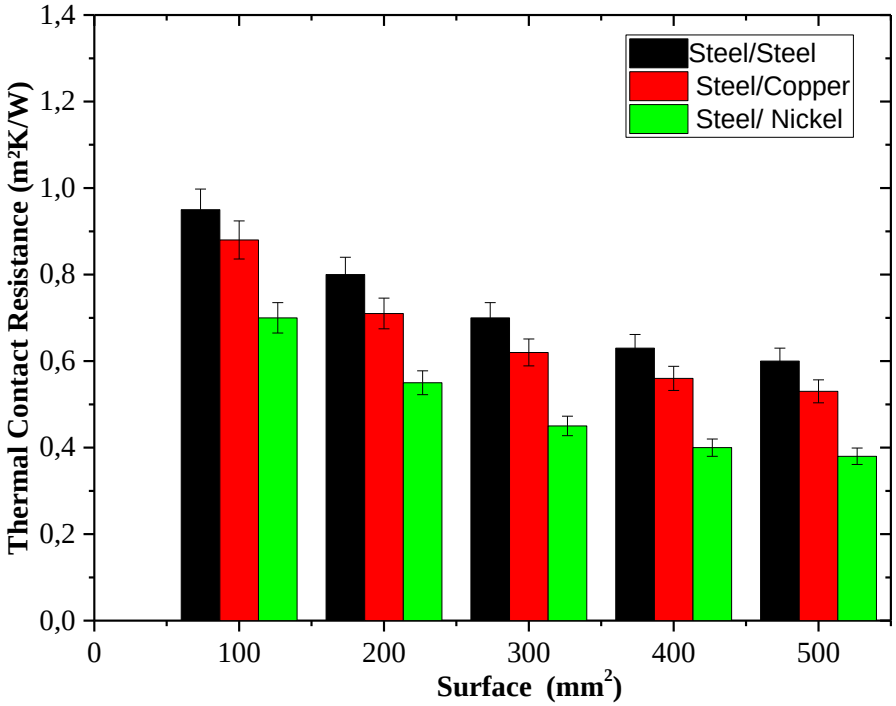

Figure 2. TCR vs surface area

3.1. Analysis of variance (ANOVA) of the TCR

The results of the variance analysis applied to contact thermal resistance are summarised in Tab. 2.

Table 2. ANOVA for Thermal Contact Resistance (TCR)

Source of variation	DDL	SS	MS	F	p-value
Material	2	0.0158	0.0079	18.45	0.002
Surface	4	0.1802	0.0451	105.23	<0.001
Interaction	8	0.0032	0.0004	0.93	0.521
Residual	15	0.0064	0.0004		
Total	29	0.2018			

The ANOVA results indicate that contact surface area has a highly significant effect on TCR ($F = 105.23$, $p < 0.001$). The material type also significantly influences TCR ($F = 18.45$, $p = 0.002$). In contrast, the material–surface interaction is not significant ($p = 0.521$), suggesting that the effect of surface area on TCR is largely independent of the specific material combination considered.

3.2. Analysis of variance (ANOVA) of heat flux

The results of the ANOVA applied to the heat flow are presented in Tab. 3.

Table 3. ANOVA for Heat Flux

Source of variation	DDL	SS	MS	F	p-value
Material	2	4.2×10^{10}	2.1×10^{10}	245.67	<0.001
Surface	4	5.8×10^{9}	1.45×10^{9}	16.92	<0.001
Interaction	8	1.2×10^{9}	1.5×10^{8}	1.75	0.167
Residual	15	1.3×10^{9}	8.67×10^{7}		
Total	29	4.91×10^{10}			

The results indicate that material type is the dominant factor influencing heat flux ($F = 245.67$, $p < 0.001$). Contact surface area also has a significant effect, though less pronounced ($F = 16.92$, $p < 0.001$). As observed for TCR, the material–surface interaction is not statistically significant, suggesting that the effects are primarily additive.

3.3. Regression model for TCR

A linear regression model was developed from the collected data to predict thermal contact resistance (TCR), expressed as follows:

$$TCR = 0.025 - 0.03S + 0.008M_{acier} + 0.002M_{nickel} \quad (14)$$

Where:

- S: contact surface (mm^2)
- M_{acier} : indicator variable for Steel/Steel
- M_{nickel} : indicator variable for Steel/Nickel

The model shows a high coefficient of determination ($R^2 = 0.96$) and an adjusted R^2 of 0.94, indicating an excellent fit to the data within the studied domain.

3.4. Validation of statistical hypotheses

The validity of the regression model was assessed using residual analyses, the results of which are presented in Tab. 4.

Table 4. Tests applied to model residues

Test	Statistique	DDL	p-value
Shapiro-Wilk	W=0.972	-	0.453
Levene	F=1.23	14.15	0.342
Durbin-Watson	DW=2.1	-	0.421

Residual analyses indicate a distribution consistent with assumptions of normality, as well as homogeneous variance, confirming the adequacy of the regression model for TCR analysis.

4. Discussion

4.1. Analysis of results and ANOVA

Fig. 2 shows a continuous reduction in TCR proportional to the increase in interfacial area for all tested material combinations. The nearly parallel trends confirm the lack of a significant material–surface interaction ($p = 0.521$, Tab. 2).

The analysis of variance indicates that contact surface area is the predominant factor, accounting for approximately 89.2% of the total TCR variance ($F = 105.23$, $p < 0.001$). This behavior can be attributed to the reduction of interfacial thermal constrictions, where the expansion of the real contact area increases the conductive pathways [26].

The absence of a significant material–surface interaction suggests that the effects of the studied parameters are mainly additive, implying that optimizing the contact surface remains a priority strategy, regardless of the selected material pair.

4.2. Material performance and microphysical interpretation

Among the studied configurations, the Steel/Copper pair consistently exhibits the lowest TCR values. This performance can be attributed to the high thermal conductivity of copper ($K \approx 400$ W/m·K) as well as its greater local deformability, which promotes an increase in the real contact area at asperities compared to the Steel/Steel pair [27].

At the microscopic scale, thermal conduction is limited by the presence of surface asperities and interfacial voids, which reduce the effective heat transfer area. The observed results, therefore, confirm that the thermomechanical properties of materials play a key role in determining thermal performance ranking [28].

From a practical perspective, these findings suggest several optimization strategies, including increasing assembly pressure and employing surface treatments such as polishing or the application of conductive coatings.

4.3. Predictive model and industrial implications

The developed regression model, characterized by a high coefficient of determination ($R^2 = 0.96$), confirms the relevance of an additive approach combining the effects of contact surface area and material type. This high predictive capability indicates that the model can reliably reproduce the trends within the studied domain.

From an industrial perspective, this model offers several immediate applications, including:

- Design of thermally dissipative interfaces, particularly in power electronics systems;
- Rational selection of the Steel/Copper pair, providing a favorable trade-off between thermal performance and cost;
- Reduction of physical testing by enabling the use of model-based simulations.

4.4. Limitations of the study and prospects

The present study primarily focuses on the effects of contact surface area and material type, while excluding other influential parameters such as surface roughness (Ra, Rq), contact pressure, and three-dimensional interfacial effects.

Future work will aim to incorporate these parameters through a multifactorial ANOVA, covering, in particular, a contact pressure range of 10–100 MPa. Extending the approach to nonlinear models based on micro-contact theory, as well as investigating the influence of thermal cycling and interfacial layers (thermal pastes or interstitial materials), will enhance the generalizability and robustness of the proposed model.

5. Conclusion

The statistical analysis proved particularly effective in characterizing the thermal performance of metal–metal junctions. The ANOVA results indicate that contact surface area is the dominant factor, accounting for 89.2% of the TCR variance ($F = 105.23$, $p < 0.001$), highlighting the importance of interfacial thermal constrictions.

The Steel/Copper pair exhibits the best thermal performance, owing to the high thermal conductivity of copper (K = 400 W/m·K) and its local malleability, which increases the real contact area. The developed linear regression model ($R^2 = 0.96$) confirms that the effects of surface area and material type are essentially additive, with the absence of a significant interaction ($p = 0.521$) underlining the robustness of this approach.

These results provide practical guidance for industrial optimization, including maximizing the effective contact area, favoring the Steel/Copper pair for a favorable performance-to-cost trade-off, and reducing reliance on prototypes through predictive numerical simulations.

Future work will aim to develop a multifactorial ANOVA incorporating surface roughness, contact pressure, and conductive interfacial layers to further enhance the predictive capability and generalizability of the model.

References

[1] Sun, D., You, E., Zhang, T., Xu, J., Wang, X., Ren, X., Tao, W., A review of thermal contact conductance research of conforming contact surfaces, Int. Commun. Heat Mass Transf., 159(B) (2024), 108065. https://doi.org/10.1016/j.icheatmasstransfer.2024.108065

[2] Chadouli, R., Makhlouf, M., Modeling of the thermal contact resistance of a solid-solid contact, IOSR J. Mech. Civ. Eng., (2014).

[3] Editorial Board, Thermal Contact Resistance, A–to–Z Guide, Feb. 2, 2011; last updated Feb. 9, 2011. https://doi.org/10.1615/AtoZ.t.thermal_contact_resistance

[4] Murwamadala, R. D., Veeredhi, V. R., Advances in thermal contact resistance studies, Proc. Inst. Mech. Eng. Part C: J. Mech. Eng. Sci., 237(1) (2023), 201–222. https://doi.org/10.1177/09544062221115297

[5] Zhao, Y., Hu, D., Li, H., Zhou, F., Li, Q., Thermal fluctuation characteristics of unsteady solid–solid interface contact heat transfer in vibration, Appl. Therm. Eng., 258(Part C) (2025), 124891. https://doi.org/10.1016/j.applthermaleng.2024.124891

[6] Xian, Y., Zhang, P., Zhai, S., Yuan, P., Yang, D., Experimental characterization methods for thermal contact resistance: A review, Appl. Therm. Eng., 130 (2018), 1530–1548. https://doi.org/10.1016/j.applthermaleng.2017.10.163

[7] Dean, A., Voss, D., Draguljić, D., Design and Analysis of Experiments, 2nd ed., Springer Cham (2017), 840 pp. https://doi.org/10.1007/978-3-319-52250-0

[8] Wei, B., Luo, W., Du, J., Ding, Y., Guo, Y., Zhu, G., Zhu, Y., Li, B., Thermal interface materials: From fundamental research to applications, SusMat, 4(6) (2024). https://doi.org/10.1002/sus2.239

[9] Pieszka Łysoń, M., Rutkowski, P., Kawalec, M., Kawalec, D., Determination of Contact Resistance of Thermal Interface Materials Used in Thermal Monitoring Systems of Electric Vehicle Charging Inlets, Mater., 17(13) (2024), 3103. https://doi.org/10.3390/ma17133103

[10] Voller, G. P., Tirovic, M., Conductive heat transfer across a bolted automotive joint and the influence of interface conditioning, Int. J. Heat Mass Transf., 50 (2007), 4833–4844. https://doi.org/10.1016/j.ijheatmasstransfer.2007.03.001

[11] Dong, Y., Zhang, P., Chen, M., Lian, W., Numerical study of thermal contact resistance considering spots and gap conduction effects, Tribol. Int., 193 (2024), 109304. https://doi.org/10.1016/j.triboint.2024.109304

[12] Mikic, B. B., Thermal contact conductance; theoretical considerations, Int. J. Heat Mass Transf., 17 (1974), 205–214. https://doi.org/10.1016/0017-9310(74)90082-9

[13] Cooper, M. G., Mikic, B. B., Yovanovich, M. M., Thermal contact conductance, Int. J. Heat Mass Transf., 12(3) (1969), 279–300. https://doi.org/10.1016/0017-9310(69)90011-8

[14] Bahrami, M., Culham, J. R., Yovanovich, M. M., Schneider, G. E., Review of Thermal Joint Resistance Models for Nonconforming Rough Surfaces, Appl. Mech. Rev., 59(1) (2006), 1–12. https://doi.org/10.1115/1.2110231

[15] Xu, R., Xu, L., An experimental investigation of thermal contact conductance of stainless steel at low temperatures, Cryogenics, 45(10–11) (2005), 694–704. https://doi.org/10.1016/j.cryogenics.2005.09.002

[16] Luo, X., Feng, H., Liu, J., Liu, S., An experimental investigation on thermal contact resistance across metal contact interfaces, Proc. 12th Int. Conf. Electron. Packag. Technol. High Density Packag. (ICEPT-HDP) (2011). https://doi.org/10.1109/ICEPT.2011.6066936

[17] Cousineau, J. E., Bennion, K. S., Chieduko, V., Lall, R., Gilbert, A., Experimental characterization and modeling of thermal contact resistance of electric machine stator-to-cooling jacket interface under interference fit loading, J. Therm. Sci. Eng. Appl., ASME, 10(4) (2018). https://doi.org/10.1115/1.4039459

[18] Madhusudana, C. V., Thermal Contact Conductance, Springer-Verlag (1996), 165 pp. ISBN:9780387945347

[19] Gao, X., Ma, J., Li, Q., Wang, M., Zan, T., Modeling of Thermal Contact Resistance of Ball Screws Considering the Load Distribution of Balls, J. Therm. Sci. Eng. Appl., 13(4) (2021), 041009. https://doi.org/10.1115/1.4048756

[20] Aalilija, A., Gandin, Ch.-A., Hachem, E., A simple and efficient numerical model for thermal contact resistance based on diffuse interface immersed boundary method, Int. J. Therm. Sci., 166 (2021), 106817. https://doi.org/10.1016/j.ijthermalsci.2020.106817

[21] Liu, Y., Yang, J., Guo, Z., Yuan, Y., Zhang, W., Wanyan, S., Numerical heat transfer analysis considering thermal contact conductance between rough reciprocating sliding surfaces, Case Stud. Therm. Eng., 65 (2025), 105580. https://doi.org/10.1016/j.csite.2024.105580

[22] Wang, Y., Sun, X., Kang, H., Ma, X., Zhang, T., Thermal contact resistance and heat transfer enhancement mechanisms at non-smooth contact interfaces, J. Therm. Sci., 34 (2025), 1–15. https://doi.org/10.1007/s11630-025-2086-5

[23] Li, Q., Chen, Z., Zhao, Y., Experimental study of influence factors on thermal contact resistance with theoretical model correlation, Int. Commun. Heat Mass Transf., 150 (2025), 109926. https://doi.org/10.1016/j.icheatmasstransfer.2025.109926

[24] Wang, J., Zhou, Y., Li, S., A peridynamic thermal contact model for heat conduction analysis of thermally imperfect interface and conductive crack, Int. J. Heat Mass Transf., 219 (2025), 126763. https://doi.org/10.1016/j.ijheatmasstransfer.2025.126763

[25] Chen, M., Hu, S., Chen, H., Zhang, P., Experimental Study of Influence Factors on Thermal Contact Resistance between Silicon Wafer and Alumina Ceramic Materials for Semiconductor Manufacturing Application, SSRN (2025). http://dx.doi.org/10.2139/ssrn.5141390

[26] Edmonds, M. J., Jones, A. M., Probert, S. D., Thermal contact resistances for hard machined surfaces pressed against relatively soft optical-flats, Appl. Energy, 6(6) (1980), 405–427. https://doi.org/10.1016/0306-2619(80)90024-0

[27] Dhuley, R. C., Pressed copper and gold-plated copper contacts at low temperatures – A review of thermal contact resistance, Cryogenics, 101 (2019), 111–124. https://doi.org/10.1016/j.cryogenics.2019.06.008

[28] Rykaczewski, K., Modeling thermal contact resistance at the finger–object interface, Temperature, 6(1) (2019), 85–95. https://doi.org/10.1080/23328940.2018.1551706

Submitted: 22.01.2026
Revised: 09.03.2026
Accepted: 02.04.2026